Scalable Coating and Properties of Transparent, Flexible, Silver Nanowire Electrodes

Liangbing Hu,[†,§] Han Sun Kim,[†,§] Jung-Yong Lee,[‡] Peter Peumans,[‡] and Yi Cui[†,*]

[†]Department of Materials Science and Engineering and [‡]Department of Electrical Engineering, Stanford University, California 94305. [§]These authors contributed equally to the work.

ABSTRACT We report a comprehensive study of transparent and conductive silver nanowire (Ag NW) electrodes, including a scalable fabrication process, morphologies, and optical, mechanical adhesion, and flexibility properties, and various routes to improve the performance. We utilized a synthesis specifically designed for long and thin wires for improved performance in terms of sheet resistance and optical transmittance. Twenty Ω/sq and ~80% specular transmittance, and 8 ohms/sq and 80% diffusive transmittance in the visible range are achieved, which fall in the same range as the best indium tin oxide (ITO) samples on plastic substrates for flexible electronics and solar cells. The Ag NW electrodes show optical transparencies superior to ITO for near-infrared wavelengths (2-fold higher transmission). Owing to light scattering effects, the Ag NW network has the largest difference between diffusive transmittance and specular transmittance when compared with ITO and carbon nanotube electrodes, a property which could greatly enhance solar cell performance. A mechanical study shows that Ag NW electrodes on flexible substrates show excellent robustness when subjected to bending. We also study the electrical conductance of Ag nanowires and their junctions and report a facile electrochemical method for a Au coating to reduce the wire-to-wire junction resistance for better overall film conductance. Simple mechanical pressing was also found to increase the NW film conductance due to the reduction of junction resistance. The overall properties of transparent Ag NW electrodes meet the requirements of transparent electrodes for many applications and could be an immediate ITO replacement for flexible electronics and solar cells.

KEYWORDS: metal nanowire · scalable coating · transparent electrode · flexible electronics · solar cells

As displays become larger and solar cells become cheaper, there is an increasing need for low-cost transparent electrodes. Various types of transparent and conductive oxides (TCO) have been widely used in optoelectronics, such as indium tin oxide (ITO), which is traditionally used for organic solar cells and light-emitting diodes, and also Al-doped ZnO, which is used in amorphous solar cells.[1] There are some emerging alternatives, such as single-walled carbon nanotubes (CNT),[2−6] graphenes,[7−16] metal or metal nanowires (NW),[17−19] and hybrids of these.[10,20,21] Owing to the mixture of carbon nanotube properties, with $^1/_3$ metallic and $^2/_3$ semiconducting, the sheet resistances of CNT electrodes are dominated by the large CNT junction resistances. A typical sheet resistance for CNT networks on plastic is 200−1000 ohms/sq with an optical transmittance of 80−90%. For voltage driven devices, such as capacitive touch screens, electrowetting displays, and liquid crystal displays, the relatively high sheet resistance of CNT networks is not problematic.[22,23] However, the relatively higher sheet resistance, compared with the *ca.* 10−50 ohms/sq of high-end ITO on plastic, would prevent the practical application of transparent CNT electrodes in current-based devices such as organic light emitting diodes and solar cells.[24] Graphene electrodes are an emerging candidate, with the best performance of ~300 ohms/sq and 80% transmittance.[20,25−27] A graphene electrode could have significantly lower cost due to the abundant material source and new methods for making thin films.[4,15,25−32] However, significant improvement is needed before the sheet resistance can reach the low values of ITO for current-driven devices. Random networks of metal NWs are a promising replacement due to its high dc conductivity and optical transmittance.[19,33] In our previous report, we demonstrated the initial performance of transparent Ag NW electrodes on glass substrates and their use in organic solar cells.[18] In a recent paper by Coleman *et al.*, the percolation behavior and DC/AC conductivity ratio for AgNW networks are studied, which was similar to a previous study for random networks of CNTs.[6,19] Here we report several new advancements in developing Ag NWs as transparent electrodes. First, higher aspect ratios of Ag NWs have been synthesized with control, which leads to the large performance improvement for

*Address correspondence to yicui@stanford.edu.

Received for review March 13, 2010 and accepted April 21, 2010.

Published online April 28, 2010.
10.1021/nn1005232

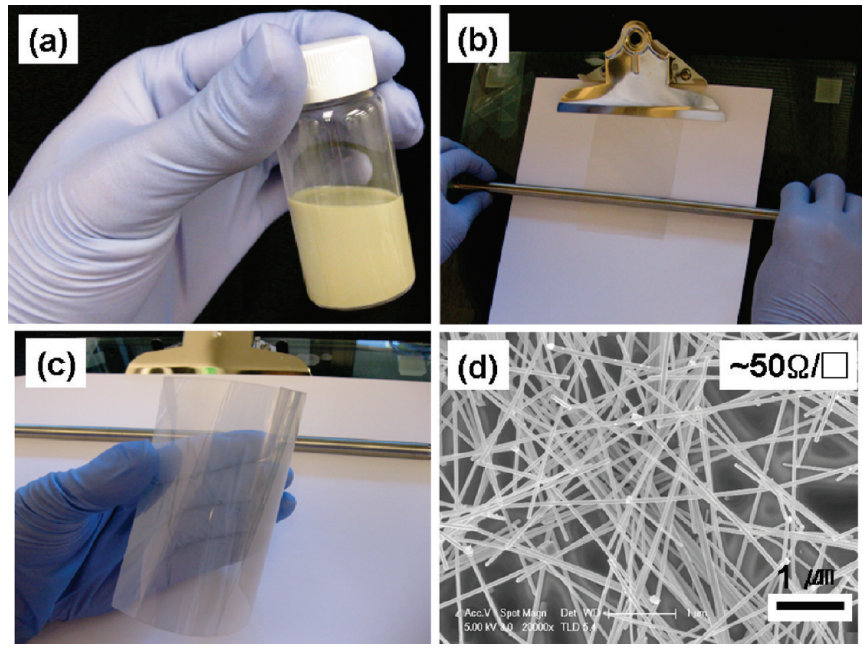

Figure 1. (a) Ag NW ink in ethanol solvent with concentration of 2.7 mg/mL. (b) Meyer rod coating setup for scalable Ag NW coating on plastic substrate. The PET plastic substrate is put on a flat glass plate and a Meyer rod is pulled over the ink and substrate, which leaves a uniform layer of Ag NW ink with thicknesses ranging from 4 to 60 μm. (c) Finished Ag NW film coating on PET substrate. The Ag NW coating looks uniform over the entire substrate shown in the figure. (d) A SEM image of Ag NW coating shown in panel c. The sheet resistance is ~50 Ω/□.

Ag NW based transparent electrodes. Second, we developed a Meyer rod coating technique for scalable roll-to-roll deposition of Ag NWs. Third, a facile electrochemical annealing method and a mechanical pressing method has been developed to reduce the NW−NW junction resistance. Fourth, we have carried out a detailed study of specular and diffusive transmittance in the near-infrared range, mechanical properties, such as adhesion and bending stability, and chemical stability.

RESULTS AND DISCUSSION

Ag NW ink is prepared as in a study by Xia *et al.* with modifications.[18,34] Figure 1a shows a 10 mL Ag NW ink in methanol solution with a concentration of 2.7 mg/mL. The ink dispersion is observed to be stable in room temperature for 3 months. After this period of time, nanowires gradually stick to each other and form irreversible clumps. To achieve uniform, agglomeration-free films, Ag inks are sonicated with a bath sonicator for 10−30 s. Figure 1b shows the Meyer rod setup for a lab scale coating of Ag NW films, which could be easily scaled-up by using slot die or graveur coating.[35] To deposit a film, 200 μL of Ag NW ink is dropped on a 120 μm thick polyethylene terephthalate (PET) substrate. Then, a Meyer rod (RDspecialist Inc.) is either pulled or rolled over the solution, leaving a uniform, thin layer of Ag NW ink on the substrate with a 4−60 μm wet thickness. The liquid thickness is solely determined by the rod wire distribution, that is, the wire diameter and the spacing. Then, the wet coating of Ag NW on PET is carefully dried using an infrared lamp. To avoid agglomeration or coffee rings, heat is applied uniformly to avoid uneven local heating. Controlled drying is critical for achieving a uniform film coating.[36] Figure 1c shows an 8 in. by 8 in. uniform coating of Ag NWs on a PET substrate. We have tested other solvents, such as ethanol and ethylene glycol (EG), and found that methanol leads to the most uniform coating. We also found that the ink concentration is important in tuning the ink viscosity optimally for uniform coatings. When the ink is diluted, the wet coating easily moves around due to the mechanical disturbance. After the initial drying of the film at 65 °C, the coating is dried at 120 °C in an oven, a step which serves as an annealing process to improve sheet conductance. The final film thickness is controlled by the ink concentration and the Meyer rod size. Figure 1d shows a Ag NW film coating on PET substrate with a sheet resistance of 50 ohms/sq.

Figure 2 shows Ag NW films with different densities on PET substrates fabricated with the simple Meyer rod coating process. As the film density increases, there are fewer holes in the films which lead to more uniform electrical field distribution when used in optoelectronic devices. By tuning the density, we can achieve ~10 ohms/sq, which meets the performance of ITO on plastic or glass substrates for solar cell and organic light emitting diode (OLED) display applications. For the Ag NWs in Figure 2, the Ag NWs are synthesized with the standard method described in the Methods section. The wire diameters are studied by SEM. As shown in Figure 2c, the diameters of Ag NWs are in the range of 40−100 nm. As shown in SEM, the holes in Ag NW network are ~200 nm for 50 ohms/sq films and bigger for sparser networks. The large openings could be problematic for

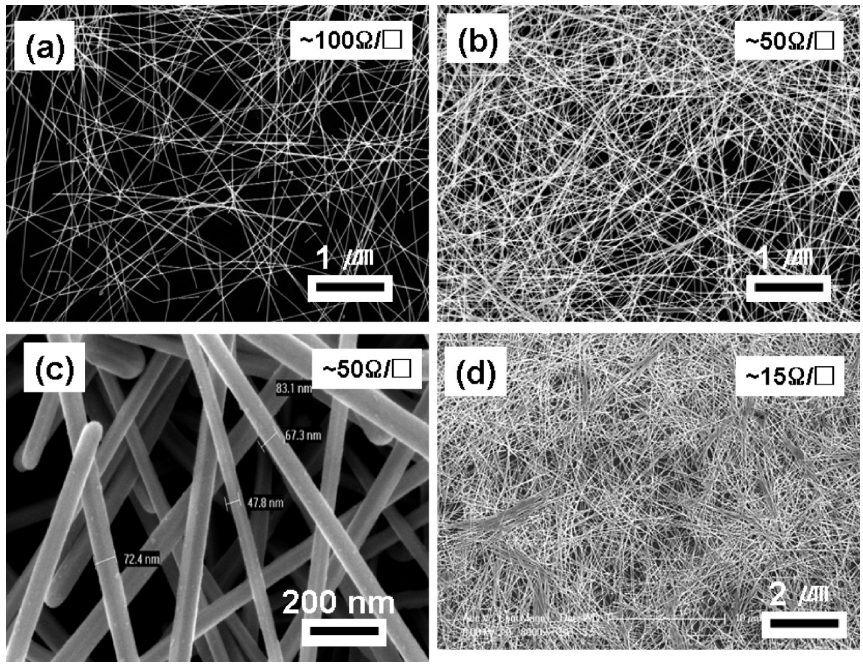

Figure 2. SEM images of Ag NW films with different densities. The different densities of Ag NW films lead to different sheet resistances: (a) 100, (b and c) 50, and (d) 15 Ω /□. The diameters of the Ag NWs are in the range of 40−100 nm.

device applications in which the charge carrier mean free path length is less than the hole size. The incorporation of other materials, such as CNTs or PEDOT, could help reduce the size of the openings for better electrical field distribution.

Optical transmittance over a large wavelength range is an important property for transparent and conductive electrodes. The transmittance is measured with a UV−vis spectrometer using a blank substrate as the reference. The transmittances for Ag NW films of several different densities are shown in Figure 3. The transmittance of an ITO-coated substrate is also shown for reference. The sheet resistance and transparency in the visible range of the Ag NW electrode are comparable to those of the ITO electrode. Furthermore, the transmittance of the Ag NW electrode is constant in the near-infrared regions, while the transmittance for the ITO electrode decreases for wavelengths >1100 nm. The decreased transmittance is due to ITO's plasma resonant wavelength at ~1300 nm, which depends on the doping level.[37] The constant transmittance of Ag NWs from 400 to 1700 nm is important for solar cells. The broad range of high transmittance in the near-infrared range also allows the Ag NW electrode to be used in infrared solar cells.[11]

The specular transmittance and the diffusive transmittance are measured for several kinds of transparent electrodes. Specular transmittance is measured by detecting only light that comes out of the sample parallel to the incident light. For our samples, this was sim-

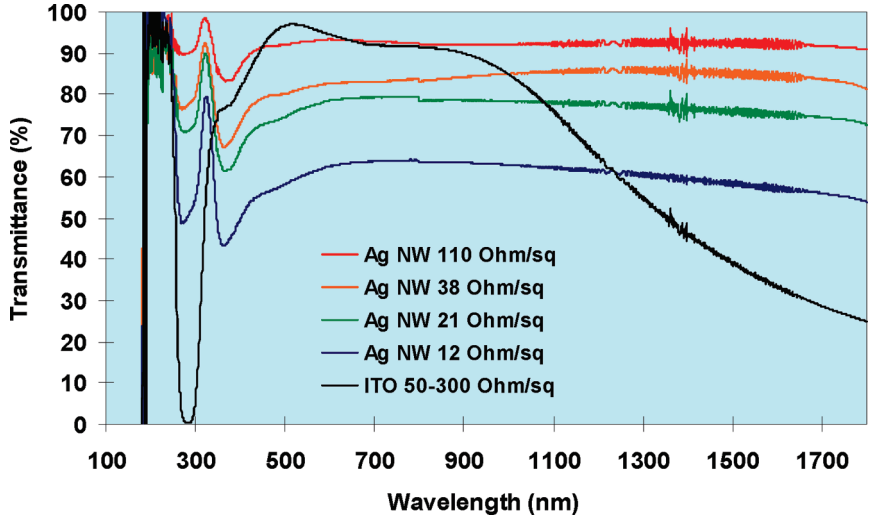

Figure 3. Optical transmittance of transparent Ag NW electrodes measured with a UV−vis spectrometer, without including the substrates. ITO on PET are obtained from CPFIlms (www.cpfilms.com).

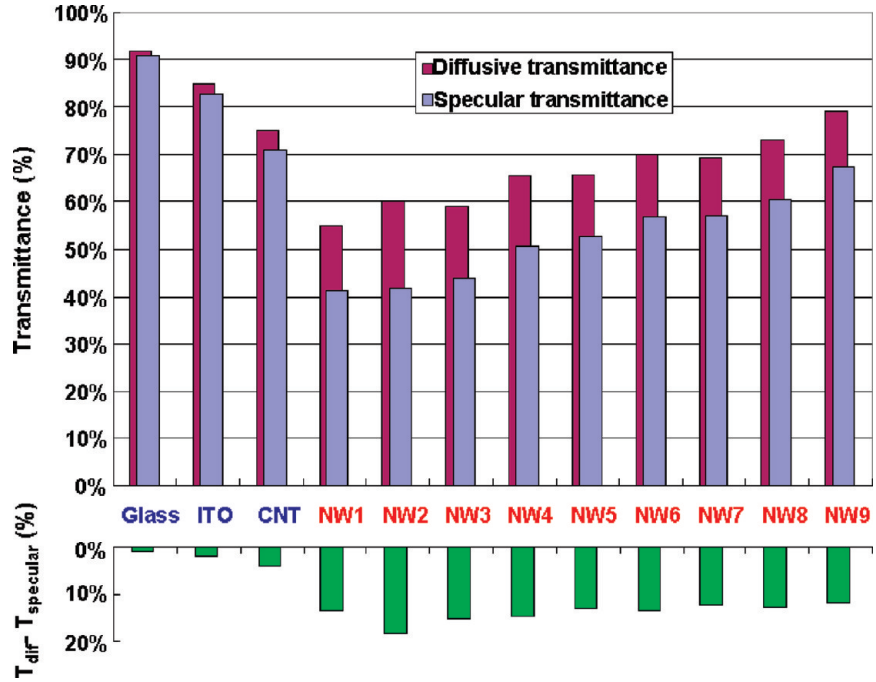

Figure 4. Diffusive and specular transmittances of glass, ITO on glass, CNT on glass, and Ag NWs with different film thicknesses on glass substrates. The differences in the diffusive transmittance and the specular transmittance are also plotted and indicate the scattering of the light by the material. The ITO substrate is from Solaronix Inc. (www.solaronix.com) with a sheet resistance of 50 ohms/sq. The CNT coating on glass is fabricated exactly according to ref 22, with sheet resistance of 120 ohms/sq.

ply measured by regular ultraviolet−visible spectroscopy in its transmittance mode. After the baseline for the spectroscopy is set by scanning a blank sample (air or glass), a sample is installed on a solid sample holder between the laser source and the photodetector. The specular and diffusive transmittance data are obtained at 500 nm wavelength. The diffusive transmittance only differs from specular transmittance in that diffusive transmittance includes all forward scattered light measured using an integrating sphere. As shown in Figure 4, the diffusive transmittance is significantly larger than the specular transmittance for Ag NW electrodes. The transmittance difference for the Ag NW electrode is ~10%, while the CNT is ~3%, and the ITO on flat substrate is ~1%. The diameter of Ag NWs is in the range of 50−100 nm, on the same order as visible light wavelength. This could lead to much more light scattering by Ag NW films compared to CNT films, since the diameter of CNTs is only a few nanometers. The large difference between diffusive transmittance and specular transmittance leads to hazy looking Ag NW electrodes, which could be problematic for certain displays such as touch screens where clear visibility is required. But it could be advantageous for certain devices used in day light where scattering is preferred. As discussed in our previous publication and others,[18,38] the large scattering of light can provide better absorption of light in solar cells, which leads to higher solar cell efficiencies. One should note that transparent CNT electrodes lose transmittance due to the absorption of visible light by CNTs while the Ag NW electrode, like thin metal films, loses transmittance due to reflection, not absorption.[2]

To be used in optoelectronic devices, transparent Ag NW electrodes must meet certain mechanical requirements to ensure device stability both during and after the fabrication process. The mechanical tape test is commonly used to assess film adhesion to the substrate. As shown in Figure 5a, the Ag NW electrode without encapsulation shows a large resistance increase after performing the tape test (3 M tape with finger pressure). This suggests that the Ag NWs have poor mechanical adhesion to the plastic substrate. By comparison, the ITO electrode shows excellent adhesion in the tape test. The adhesion of Ag NWs to the plastic substrate can be largely improved by encapsulation, using a thin layer of organic materials. We demonstrate this using 20 nm of Teflon to encapsulate the electrode. After encapsulating the Ag NW film with Teflon, it shows only a small sheet resistance increase after the tape test. Another important test for plastic electronics and solar cells is the flexibility test. ITO on PET is well-known to have poor flexibility, as shown in Figure 5b. However, the Ag NW electrode shows outstanding robustness upon being bent down 100 times to 5 mm with and without encapsulation. For incorporation of this transparent and conductive electrode into practical devices, the electrode also needs to be resistant to chemical damage and heat. This will ensure that the electrode can survive the device manufacturing process and not limit long-term stability of the device. The standard specification for these tests is that the change in sheet

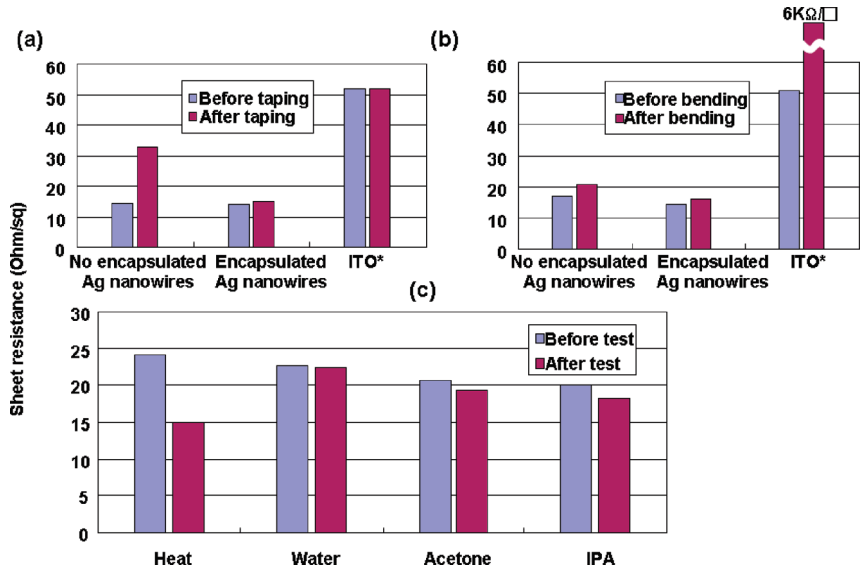

Figure 5. Mechanical and chemical stability of Ag NW films on plastic substrates. (a) The sheet resistances of Ag NW films and ITO on PET before and after a taping test. When the Ag NW film is encapsulated with 20 nm Teflon, the taping test result shows a much smaller resistance increase. (b) Bending test of Ag NW films, with and without encapsulation, and ITO on a PET substrate. Ag NW electrodes show much better bending properties. (c) The sheet resistance changes of Ag NWs after exposure to heat (120 C for 123 h), water for 10 min, acetone for 10 min, and IPA for 10 min. Ag NW films on PET substrates show excellent resistances to exposure.

resistance, $\Delta R_s/R_s$ be less than 30%. This requirement varies for different device applications and companies.[39] The sheet resistance increases less than 5% for both encapsulated and unencapsulated Ag NW electrodes when left in air for one month. We choose to test the resistance of the Ag NW electrode against heat, water, acetone, and IPA exposure, which are standard tests from touch screen manufacturing.[40] Surprisingly, Ag NW electrodes show almost no change when exposed to water, acetone, and IPA, and show decrease of sheet resistance when exposed to heat at 120 C for 123 h. Possible explanations for the sheet resistance decrease upon prolong heating are that (1) the junction conductance between Ag NWs is improved due to the continuing removal of the PVP residues between Ag NWs or (2) the contact between NW to substrates is improved due to heating, which improves the NW network morphology and the electrical contacts between wires. The outstanding stability of the Ag NW electrode is further evidence that it is ready for utilization in devices.

For use in large scale displays and solar cells, low resistance is always required. There are studies for transparent electrodes based on solution-processed CNT films that indicate smaller bundles and longer CNTs improve electrode performance.[23] The same idea can be applied to Ag NW electrodes. The longer and thinner nanowires would significantly decrease the percolation threshold in surface conductance.[6] We use the addition of KBr solution during the synthesis to grow longer and thinner wires (Figure 6a). The details can be found in the Methods section. Figure 6b shows the SEM images of Ag NWs with the standard recipe (left) and the modified recipe (right). The modified recipe produces ~50% thinner Ag NWs. The diameters of Ag NWs for the standard recipe are 50−100 nm and 30−50 nm for the modified recipe. We evaluated the performance of the two types of Ag NWs in electrodes and compared them to typical ITO, graphene, and CNT electrodes.[26,41] We find that the thin/longer wires increase the optical transmittance at the same sheet resistance compared to the regular wires (Figure 6c). The performance of ITO on plastic is based on ITO from CPFilms Inc. Each Ag NW electrode was prepared by Meyer rod coating on glass, followed by annealing and pressing without gold coating. Typical performance for thinner Ag NWs is 20 ohms/sq sheet resistance and 80% specular transmittance at 500 nm. For display applications, the specular transmittance of the Ag NW electrode demonstrated here already meets all the application requirements. For use in solar cells, the diffusive transmittance should be used. From Figure 6c, ~8 ohms/sq sheet resistance and 65% specular transmittance is achieved. The difference between diffusive transmittance and specular transmittance for the film is typically ~15%, as shown in Figure 4. Therefore, ~8 ohms/sq sheet resistance and 80% diffusive transmittance is obtained, which is sufficient for using transparent Ag NW electrodes in solar cells. The sparseness of the network, with the hole sizes up to ~1 μm, would be problematic if the charge diffusion length is less than the hole size. This problem would be overcome by a top coating of another layer of conductive materials, such as PEDOT:PSS or a carbon nanotube network to fill the holes. The work function of a Ag NW electrode could also be modified by coating another layer of materials.[18,42] Our recent work demon-

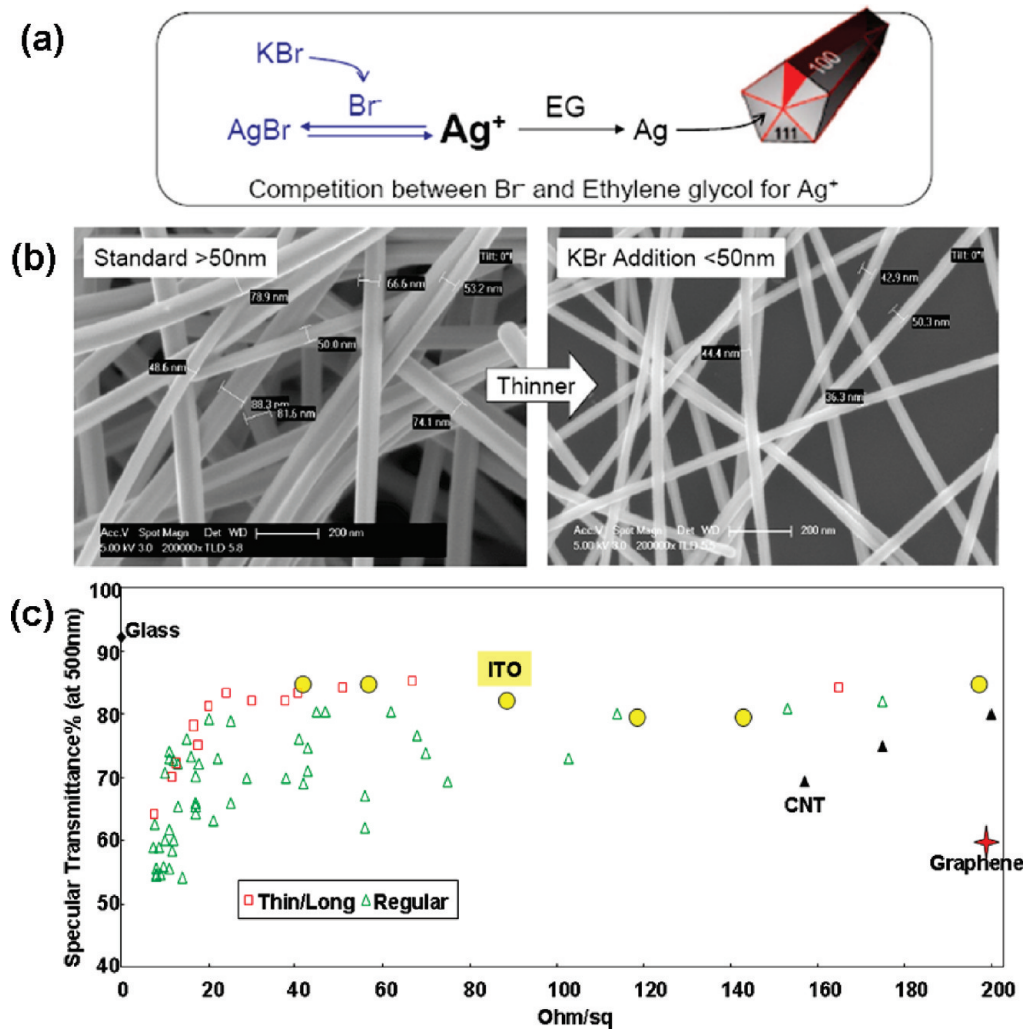

Figure 6. (a) Schematic to show that the competition between Br- and ethylene glycol for Ag^+ retards the supply of silver atoms and results in more effective anisotropic growth of the nanowires. (b) SEM confirms that the addition of KBr helps grow longer and thinner wires, from 50−100 nm to 30−50 nm. (c) Transmittance at 500 nm and sheet resistances for Ag NW electrodes based on regular NWs and thin/long wires with KBr addition in the NW preparation step. The performance of ITO, CNT, and graphene are shown for comparison.

strated that Ag NW electrodes can be used as either anode or cathode.[43] Our solar cell performance indicates that the Ag NWs are chemically stable when in contact with the solar cell active layer. We did not perform stability test under extended-time UV exposure, but we believe this is not going to cause any issues since Ag NWs are well buried under the active layer materials and encapsulated properly. Overall, performances of the thinner/longer nanowires are much better than those of regular wires, and the performances of the thinner/long nanowires are comparable to the best ITO on plastic substrate device and much better than CNT electrodes.

For the Ag NW electrode, the charge transport mainly includes two components: along the wires and across the junctions. To determine which is limiting the conductivity of the Ag NW electrodes, we measured the single NW resistance and the NW−NW junction resistance. Figure 7a shows the SEM of two Ag NWs under the silver contacts for electrical measurements. These silver contacts were deposited by E-beam lithography and allow us to measure the resistance along each Ag NW and the junction resistances. The resistances of the two Ag NWs are 260 and 320 ohms, respectively, and the junction resistance is larger than 1 GΩ. Another method to increase the conductivity is to decrease the junction resistance between the NWs. We found that Au replacement is an effective method to do this. The Au coating process is as follows. A 1.3 cm by 1.9 cm piece of AgNW film is immersed for 15 min in a boiling 0.007 mM $HAuCl_4$ aqueous solution. Then, the film is taken out of the solution and dried with an air gun. This simple process of Galvanic displacement turns the network of pure Ag NWs into a network of gold-coated Ag NWs, which are silver−gold alloyed nanowires, with rough surfaces and some dangling nanoparticles. After Au coating, the wire resistances of the same pair of Ag NWs slightly decrease to 220 and 300 ohms, respectively, while the junction resistance drastically decreases to 450 ohms. Figure 7b illustrates the coating

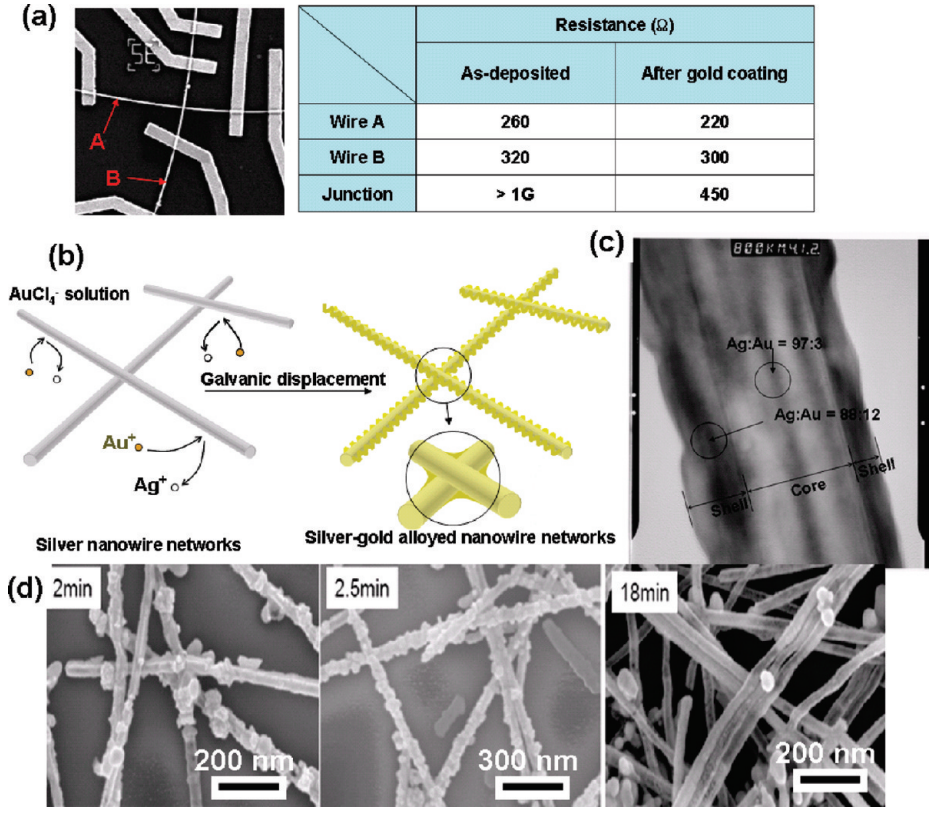

	Resistance (Ω)	
	As-deposited	After gold coating
Wire A	260	220
Wire B	320	300
Junction	> 1G	450

Figure 7. (a) Electrical measurement of individual Ag NWs and a junction. The junction shows much higher resistances than those of the wires themselves. The junction resistance dramatically decreases from >1 GΩ to 450 Ω after the Au coating. The lengths of the two wires are ~10 μm each. (b) Schematic of Au−Ag alloy network formation by the solution process. (c) TEM image showing the nanowire after the Au replacement. (d) Au replacement with different Au addition time. The surface of nanowires is smoother when Au is supplied more slowly.

process. The transmission electron microscopy (TEM) image in Figure 7c shows the presence of Au in the wire after Au coating. The image was taken on an FEI CM20 TEM at the Stanford Nanocharacterization Laboratory. Energy dispersive spectroscopy (EDS) was performed on the same instrument with a spot size estimated to be ~20 nm. The sample was prepared by drop-casting a dispersion of the gold-coated silver nanowires in methanol onto a Formvar-coated copper grid and allowing it to dry in air for 1 h. It is clear that the Ag NW has a large amount of Au on the surface after Au coating. We found that the Au coating decreases the overall electrode film resistance from several thousands ohms/sq to several tens ohms/sq, which is mainly due to the change in junction resistance, as verified by the junction resistance measurement. The surface morphologies of Ag−Au alloyed nanowires can be controlled by the titration rate of $HAuCl_4$. Smoother surfaces can be achieved when slower titration is used (Figure 7d).

We also tested mechanical pressure as a means to improve electrode performance by decreasing the junction resistance in order to decrease the sheet resistance. A pair of clean glass slides together with a Ag NW electrode film are sandwiched between two steel plates. The steel plates are then pressed by a mechanical manual presser up to 81 GPa pressure, held for 50 s, and released. The SEM image (Figure 8a) shows the surface of the Ag NW electrode after mechanical pressing.

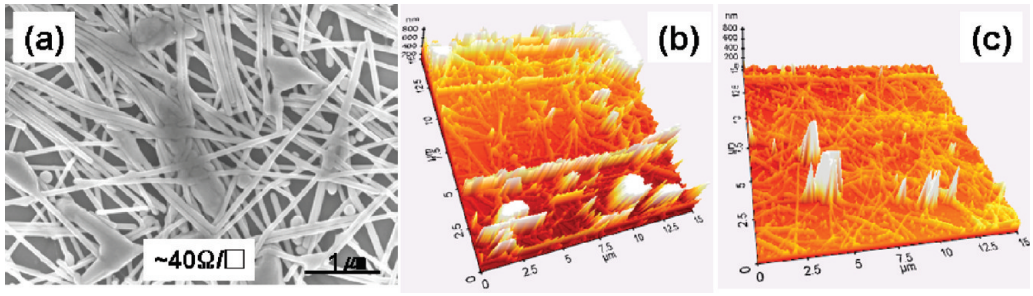

Figure 8. (a) SEM of Ag NW network after mechanical press; AFM images of the Ag NW network (b) before and (c) after pressing. The pressing significantly improves the smoothness. The surface roughness decreases from 110 to 47 nm after mechanical pressing.

The sheet resistance typically decreases from several hundreds ohms/sq to several tens ohms/sq. The mechanical pressing not only increases the conductance but also greatly improves the film morphology. AFM shows that the surface roughness of the Ag NW electrode decreases greatly after pressing (Figure 8b,c). The surface roughness decreases from 110 to 47 nm after pressing. The surface roughness is extremely important for use of Ag NW electrodes in OLEDs, in which 1−2 nm surface roughness is typically required.[44] This could be achieved by encapsulation of a Ag NW electrode with conducting polymers to fill the holes in the film.

CONCLUSION

We present a comprehensive characterization of Ag NW transparent electrodes, beginning with the material synthesis. We demonstrate size control of Ag NWs, in particular their lengths and diameters. The Ag NWs are highly conductive, and the resistances of Ag NWs with lengths ~10 μm are ~200−300 Ω for the individual wires and ~450 Ω for wire−wire junctions. The Meyer rod coating method was successfully applied to fabricate Ag NW films on plastic substrates. This method is widely used in industry and can be scaled up to a roll-to-roll process. Twenty Ω/sq, ~80% specular transmittance, and 8 ohms/sq and 80% diffusive transmittance in the visible spectral range were achieved, which out-performs most ITO electrodes on plastic substrates and the best CNT or graphene networks. The transmittance spectrum is much flatter than that for ITO in the visible and near-infrared range. A large portion of light is scattered in Ag NW electrodes, up to 20%, which is much larger than the ITO and the CNT electrode. This could be beneficial for solar cell applications. The Ag NW coating on plastic passes both chemical and environmental stability tests. The outstanding flexibility makes the Ag NW electrode attractive for flexible electronics. Furthermore, various approaches to further improve the performance of the Ag NW electrodes, such as using thin/long nanowires, gold coating, and pressing to increase the junction conductance were demonstrated. We believe that transparent electrodes based on Ag NWs can be immediately utilized in plastic electronics and high-efficiency solar cells.

METHODS

Synthesis. Ag NWs are synthesized in solution as follows. A mixture of 0.334 g PVP (poly vinylpyrrolidone) and 20 mL EG (ethylene glycol) is heated and thermally stabilized at 170 °C in a flask; 170 °C is a high enough temperature to enhance the reducing power of EG and is below the boiling temperature of EG (197.3 °C). Once the temperature has been stabilized, 0.025 g of silver chloride (AgCl) is ground finely and added to the flask for initial nucleation of the silver seeds. After three minutes, 0.110 g of silver nitrate ($AgNO_3$), the actual silver source, is titrated for 10 min. The reason for the slow addition is that it is not desirable to create various shapes of nanostructures, such as spheres, cubes, or rods by excessively facilitating the crystal growth. After enough of the silver sources have been supplied, the flask is heated for an additional 30 min to ensure that the growth is complete. The cooled-down solution is then centrifuged three times at 6000 rpm for 30 min to remove solvent (EG), PVP, and other impurities in the supernatant. After the final centrifuge, the precipitate of AgNWs is redispersed in 30 mL of methanol.

The detailed synthesis for growing longer and thinner Ag NW is as follows. First, a mixture of 0.668 g of PVP (poly vinylpyrrolidone), 0.010 g of KBr (potassium bromide), and 20 mL of EG (ethylene glycol) is heated and thermally stabilized at 170 °C in a flask. Next, 0.050 g of silver chloride (AgCl) is ground finely and added to the flask for initial nucleation of the silver seeds. After 3 min, 0.220 g of silver nitrate ($AgNO_3$) is titrated for 10 min. Then, the flask is heated for additional 30 min to ensure that the growth is complete. The cooled-down solution is then centrifuged at 2000 rpm for 30 min to isolate the long/thin wires, which remain in the supernatant. Then, the supernatant containing the long/thin wires is centrifuged twice at 6000 rpm for 30 min to precipitate the wires. We discard the supernatant containing solvent (EG), PVP, and other impurities. After the final centrifuge, the precipitate of Ag NWs is dispersed in 5 mL of methanol. It is noticeable that the longer/thinner wire solution is less concentrated than the solution from the regular synthesis for the same volume of solvent. This is because this longer/thinner wire recipe generates numerous big silver particles, which are removed during centrifugation.

Sheet Resistance Measurement. Square silver contacts with thicknesses more than 80 nm are deposited on an Ag NW film by a thermal evaporator. The mask for the evaporator is designed in a way such that the exposed area between the two silver pads is a perfect square. (e.g., same vertical and horizontal lengths) The Ag NWs beyond the silver pads and the area between are removed. The sheet resistance of the Ag NW film is just identical to the bulk resistance between the two silver pads, when those silver pads are assumed to be infinitely conductive.

Encapsulation. Telfon encapsulation is done using the Meyer rod coating method. A piece of the AgNW coated film is placed on the Meyer rod apparatus, and then several drops of Teflon adhesive solution are dropped on it. Immediately afterward, the Meyer rod is rolled over the drops to spread the Teflon solution evenly over the AgNW film. By heating the film at 120 °C for 10 min, the thin Teflon layer is cured solid.

SEM and AFM. All the SEM images were taken on the FEI XL30 Sirion SEM with FEG source at the Stanford Nanocharacterization Laboratory. The AFM system used was a Park Systems XE-70 SPM and was operated in noncontact mode.

Acknowledgment. The authors acknowledge support from the King Abdullah University of Science and Technology (KAUST) Investigator Award (No. KUS-I1-001-12), Stanford Global Climate and Energy Projects, and U.S. Department of Energy. The authors also acknowledge some experimental help from Steve Connor and Chong Xie.

REFERENCES AND NOTES

1. Gordon, R. G. Criteria for Choosing Transparent Conductors. *MRS Bull.* **2000**, *25*, 52–57.
2. Hu, L.; Hecht, D. S.; Gruner, G. Carbon Nanotube Thin Films: Fabrications, Properties and Applications. Chem. Rev. In press.
3. Dan, B.; Irvin, G. C.; Pasquali, M. Continuous and Scalable Fabrication of Transparent Conducting Carbon Nanotube Films. *ACS Nano* **2009**, *3*, 835–843.
4. Cao, Q.; Zhu, Z. T.; Lemaitre, M. G.; Xia, M. G.; Shim, M.; Rogers, J. A. Transparent Flexible Organic Thin-Film Transistors That Use Printed Single-Walled Carbon Nanotube Electrodes. *Appl. Phys. Lett.* **2006**, *88*, 113511.
5. Wu, Z. C.; Chen, Z. H.; Du, X.; Logan, J. M.; Sippel, J.; Nikolou, M.; Kamaras, K.; Reynolds, J. R.; Tanner, D. B.;

Hebard, A. F.; Rinzler, A. G. Transparent, Conductive Carbon Nanotube Films. *Science* **2004**, *305*, 1273–1276.
6. Hu, L.; Hecht, D. S.; Gruner, G. Percolation in Transparent and Conducting Carbon Nanotube Networks. *Nano Lett.* **2004**, *4*, 2513–2517.
7. Becerril, H. A.; Mao, J.; Liu, Z.; Stoltenberg, R. M.; Bao, Z.; Chen, Y. Evaluation of Solution-Processed Reduced Graphene Oxide Films as Transparent Conductors. *ACS Nano* **2008**, *2*, 463–470.
8. Eda, G.; Lin, Y. Y.; Miller, S.; Chen, C. W.; Su, W. F.; Chhowalla, M. Transparent and Conducting Electrodes for Organic Electronics from Reduced Graphene Oxide. *App Phys. Lett.* **2008**, *92*, 233305.
9. Geim, A. K.; Novoselov, K. S. The Rise of Graphene. *Nat. Mater.* **2007**, *6*, 183–191.
10. Hong, W. J.; Xu, Y. X.; Lu, G. W.; Li, C.; Shi, G. Q. Transparent Graphene/PEDOT-PSS Composite Films as Counter-Electrodes of Dye-Sensitized Solar Cells. *Electrochem. Commun.* **2008**, *10*, 1555–1558.
11. Hu, L. B.; Hecht, D. S.; Gruner, G. Infrared Transparent Carbon Nanotube Thin Films. *Appl. Phys. Lett.* **2009**, *94*, 081103.
12. Li, X. L.; Zhang, G. Y.; Bai, X. D.; Sun, X. M.; Wang, X. R.; Wang, E.; Dai, H. J. Highly Conducting Graphene Sheets and Langmuir−Blodgett Films. *Nat. Nanotechnol.* **2008**, *3*, 538–542.
13. Meyer, J. C.; Geim, A. K.; Katsnelson, M. I.; Novoselov, K. S.; Booth, T. J.; Roth, S. The Structure of Suspended Graphene Sheets. *Nature* **2007**, *446*, 60–63.
14. Son, Y. W.; Cohen, M. L.; Louie, S. G. Energy Gaps in Graphene Nanoribbons. *Phys. Rev. Lett.* **2006**, *97*, 216803.
15. Wang, X.; Zhi, L. J.; Mullen, K. Transparent, Conductive Graphene Electrodes for Dye-Sensitized Solar Cells. *Nano Lett.* **2008**, *8*, 323–327.
16. Wu, J. B.; Becerril, H. A.; Bao, Z. N.; Liu, Z. F.; Chen, Y. S.; Peumans, P. Organic Solar Cells with Solution-Processed Graphene Transparent Electrodes. *Appl. Phys. Lett.* **2008**, *92*, 263302.
17. Ju, S.; Li, J. F.; Liu, J.; Chen, P. C.; Ha, Y. G.; Ishikawa, F.; Chang, H.; Zhou, C. W.; Facchetti, A.; Janes, D. B.; Marks, T. J. Transparent Active Matrix Organic Light-Emitting Diode Displays Driven by Nanowire Transistor Circuitry. *Nano Lett.* **2008**, *8*, 997–1004.
18. Lee, J. Y.; Connor, S. T.; Cui, Y.; Peumans, P. Solution-Processed Metal Nanowire Mesh Transparent Electrodes. *Nano Lett.* **2008**, *8*, 689–692.
19. De, S.; Higgins, T. M.; Lyons, P. E.; Doherty, E. M.; Nirmalraj, P. N.; Blau, W. J.; Boland, J. J.; Coleman, J. N. Silver Nanowire Networks as Flexible, Transparent, Conducting Films: Extremely High DC to Optical Conductivity Ratios. *ACS Nano* **2009**, *3*, 1767–1774.
20. Tung, V. C.; Allen, M. J.; Yang, Y.; Kaner, R. B. High-Throughput Solution Processing of Large-Scale Graphene. *Nat. Nanotechnol.* **2009**, *4*, 25–29.
21. Tung, V. C.; Chen, L. M.; Allen, M. J.; Wassei, J. K.; Nelson, K.; Kaner, R. B.; Yang, Y. Low-Temperature Solution Processing of Graphene-Carbon Nanotube Hybrid Materials for High-Performance Transparent Conductors. *Nano Lett.* **2009**, *9*, 1949–1955.
22. Hu, L. B.; Gruner, G.; Gong, J.; Kim, C. J.; Hornbostel, B. Electrowetting Devices with Transparent Single-Walled Carbon Nanotube Electrodes. *Appl. Phys. Lett.* **2007**, *90*, 093124.
23. Hecht, D.; Hu, L.; Gruner, G. Conductive Scaling of CNTs. *Appl. Phys. Lett.* **2006**, *89*, 133122.
24. Rowell, M. W.; Topinka, M. A.; McGehee, M. D.; Prall, H. J.; Dennler, G.; Sariciftci, N. S.; Hu, L. B.; Gruner, G. Organic Solar Cells with Carbon Nanotube Network Electrodes. *Appl. Phys. Lett.* **2006**, *88*, 233506.
25. Eda, G.; Fanchini, G.; Chhowalla, M. Large-Area Ultrathin Films of Reduced Graphene Oxide as a Transparent and Flexible Electronic Material. *Nat. Nanotechnol.* **2008**, *3*, 270–274.
26. Wu, J. B.; Agrawal, M.; Becerril, H. A.; Bao, Z. N.; Liu, Z. F.; Chen, Y. S.; Peumans, P. Organic Light-Emitting Diodes on Solution-Processed Graphene Transparent Electrodes. *ACS Nano* **2009**, *4*, 43–48.
27. Xuan, W.; Linjie, Z.; Mullen, K. Transparent, Conductive Graphene Electrodes for Dye-Sensitized Solar Cells. *Nano Lett.* **2008**, *8*, 323.
28. De, S.; Coleman, J. N. Are There Fundamental Limitations on the Sheet Resistance and Transparent of Thin Graphene Films? ACS Nano, published online April 12, 2010, http://doi.dx.org/10.1021/nn100343f.
29. Kim, K. S.; Zhao, Y.; Jang, H.; Lee, S. Y.; Kim, J. M.; Kim, K. S.; Ahn, J.-H.; Kim, P.; Choi, J.-Y.; Hong, B. H. Large-Scale Pattern Growth of Graphene Films for Stretchable Transparent Electrodes. *Nature* **2009**, *457*, 706–710.
30. Li, X. S.; Zhu, Y. W.; Cai, W. W.; Borysiak, M.; Han, B. Y.; Chen, D.; Piner, R. D.; Colombo, L.; Ruoff, R. S. Transfer of Large-Area Graphene Films for High-Performance Transparent Conductive Electrodes. *Nano Lett.* **2009**, *9*, 4359–4363.
31. Reina, A.; Jia, X. T.; Ho, J.; Nezich, D.; Son, H. B.; Bulovic, V.; Dresselhaus, M. S.; Kong, J. Large Area, Few-Layer Graphene Films on Arbitrary Substrates by Chemical Vapor Deposition. *Nano Lett.* **2009**, *9*, 30–35.
32. Hernandez, Y.; Nicolosi, V.; Lotya, M.; Blighe, F. M.; Sun, Z. Y.; De, S.; McGovern, I. T.; Holland, B.; Byrne, M.; Gun'ko, Y. K.; *et al*. High-Yield Production of Graphene by Liquid-Phase Exfoliation of Graphite. *Nat. Nanotechnol.* **2008**, *3*, 563–568.
33. Azulai, D.; Belenkova, T.; Gilon, H.; Barkay, Z.; Markovich, G. Transparent Metal Nanowire Thin Films Prepared in Mesostructured Templates. *Nano Lett.* **2009**, *9*, 4246–4249.
34. Sun, Y.; Gates, B.; Mayers, B.; Xia, Y. Crystalline Silver Nanowires by Soft Solution Processing. *Nano Lett.* **2002**, *2*, 165.
35. Tracton, A. A. *Coatings Technology Handbook*; Marcel Dekker Inc: New York, 2005.
36. Gutoff, E. B.; Cohen, E. D. *Coating and Drying Defects: Troubleshooting Operating Problems*; John Wiley & Sons Inc: New York, 2006.
37. Ginley, D. S.; Bright, C. Transparent conducting oxides. *MRS Bull.* **2000**, *25*, 15–18.
38. Atwater, H. A.; Polman, A. Plasmonics for improved photovoltaic devices. *Nat. Mater.* **2010**, *9*, 205–213.
39. TouchKit. www.touchkit.com. Accessed April 26, 2010.
40. Hecht, D. S.; Thomas, D.; Hu, L.; Ladous, C.; Lam, T.; Park, Y.; Irvin, G.; Drzaic, P. Carbon-Nanotube Film on Plastic as Transparent Electrode for Resistive Touch Screens. *J. Soc. Inf. Displ.* **2009**, *17*, 941.
41. Li, J.; Hu, L.; Wang, L.; Zhou, Y.; Gruner, G.; Marks, T. J. Organic Light-Emitting Diodes Having Carbon Nanotube Anodes. *Nano Lett.* **2006**, *6*, 2472–2477.
42. Gaynor, W.; Lee, J. Y.; Peumans, P. Fully Solution-Processed Inverted Polymer Solar Cells with Laminated Nanowire Electrodes. *ACS Nano* **2010**, *4*, 30–34.
43. Lee, J.-Y.; Connor, S. T.; Cui, Y.; Peumans, P. Semitransparent Organic Photovoltaic Cells with Laminated Top Electrode. *Nano Lett.* **2010**, *10*, 1276.
44. Müllen, K. Scherf, U. *Organic Light Emitting Devices: Synthesis, Properties and Applications*: Wiley-VCH Verlag: Weinheim, Germany, 2006.